Journal of Structural Geology 31 (2009) 1183–1196

Contents lists available at ScienceDirect

Journal of Structural Geology

journal homepage: www.elsevier.com/locate/jsg

Shock effects and pre-shock microstructures in hydrothermal quartz veins from the Rochechouart impact structure, France

C.A. Trepmann

Institut für Geologie, Mineralogie und Geophysik, Ruhr-Universität Bochum, Universitätsstraße 150, Sonderforschungsbereich 526, D-44801 Bochum, Germany

ARTICLE INFO

Article history:
Received 2 February 2009
Received in revised form
18 May 2009
Accepted 28 June 2009
Available online 8 July 2009

Keywords:
Shock effects
Microstructure
High stress deformation
Recrystallization
Quartz

ABSTRACT

Microfabrics in hydrothermal quartz veins in gneisses of the Massif Central, France, from the Rochechouart impact structure and *St. Paul la Roche*, ~40 km to the SE of the centre of the structure, have been investigated. In the quartz veins from the Rochechouart impact structure, planar deformation features in the basal plane and cataclastic zones indicate low shock pressures (<*c.* 8 GPa), and high shock-induced differential stresses. Recrystallized grains, subgrains and undulating deformation lamellae are interpreted as pre-shock features. In quartz veins from *St. Paul la Roche* outside the impact structure no shock effects occur. There, the microfabric is characterized by healed microcracks, undulating deformation lamellae, subgrains and recrystallized grains aligned along fractures. These microstructures are similar to the pre-shock features of quartz veins within the impact structure. They indicate initial high stress glide-controlled deformation accompanied by microcracking and subsequent modification by recovery and recrystallization at low stress. Such a microfabric development is characteristic for coseismic loading and postseismic stress relaxation in the middle crust below the seismogenic layer. The microfabric of the *St. Paul la Roche* quartz vein is considered as potential "starting material" for the deformation of quartz veins during the late Triassic meteorite impact at Rochechouart.

1. Introduction

Microstructures resulting from deformation and mineral transformations induced by ultra-high pressures as a result of a shock wave, which is generated by a meteorite impact, are termed shock effects. They can give important information on the conditions prevailing during impact cratering (e.g., Langenhorst and Deutsch, 1994; Stöffler and Langenhorst, 1994; Grieve et al., 1996; French, 1998). To realize this information, a distinction between shock effects and pre- or post-shock microstructures is crucial. Shock effects, as diaplectic glass, mosaicism and planar deformation features (PDFs) parallel to rhombohedral planes, are clearly distinct from any microstructures generated at continuous and slow rate tectonic deformation. These shock effects are assumed to develop by a transformation into a high-density amorphous phase during shock compression at high quasi-hydrostatic pressure and subsequent decompression and without the involvement of shear deformation (e.g., Goltrant et al., 1992; Langenhorst, 1994; Stöffler and Langenhorst, 1994; Grieve et al., 1996; French, 1998). Rhombohedral PDFs are prominent shock effects in quartz that are formed by a discontinuous and localized transformation along various rhombohedral planes (mostly $\boldsymbol{\pi}$, $\boldsymbol{w}$ rhombohedra) and are commonly annealed resulting in multiple sets of rhombohedral planes that are decorated by dislocations and fluid inclusions (Goltrant et al., 1992; Leroux et al., 1994; Leroux and Doukhan, 1996). However, the differentiation of microstructures derived from impactites at some distance from the centre of an impact structure at attenuated shock pressure (Trepmann and Spray, 2006; Trepmann, 2008) on the one hand, from microstructures developed during short-term high stress deformation, e.g., related to seismic faulting on the other (e.g., Küster and Stöckhert, 1999; Trepmann and Stöckhert, 2001, 2002, 2003; Nüchter and Stöckhert, 2008) is less apparent. Both originate from strongly non-steady state deformation at a high rate of loading and undergo subsequent modification at low stress.

At the Rochechouart impact structure, France (Fig. 1), the microfabrics in quartz veins show both, shock effects and evidence of short-term high stress pre-shock deformation. The intensity of this pre-shock and shock-induced deformation, however, is highly variable. In the present study, microstructures in quartz veins from the Rochechouart impact structure and those in the quartz vein from *St. Paul la Roche*, about 40 km from the centre of the impact structure, are compared.

E-mail address: claudia.trepmann@rub.de

0191-8141/$ – see front matter © 2009 Elsevier Ltd. All rights reserved.
doi:10.1016/j.jsg.2009.06.017

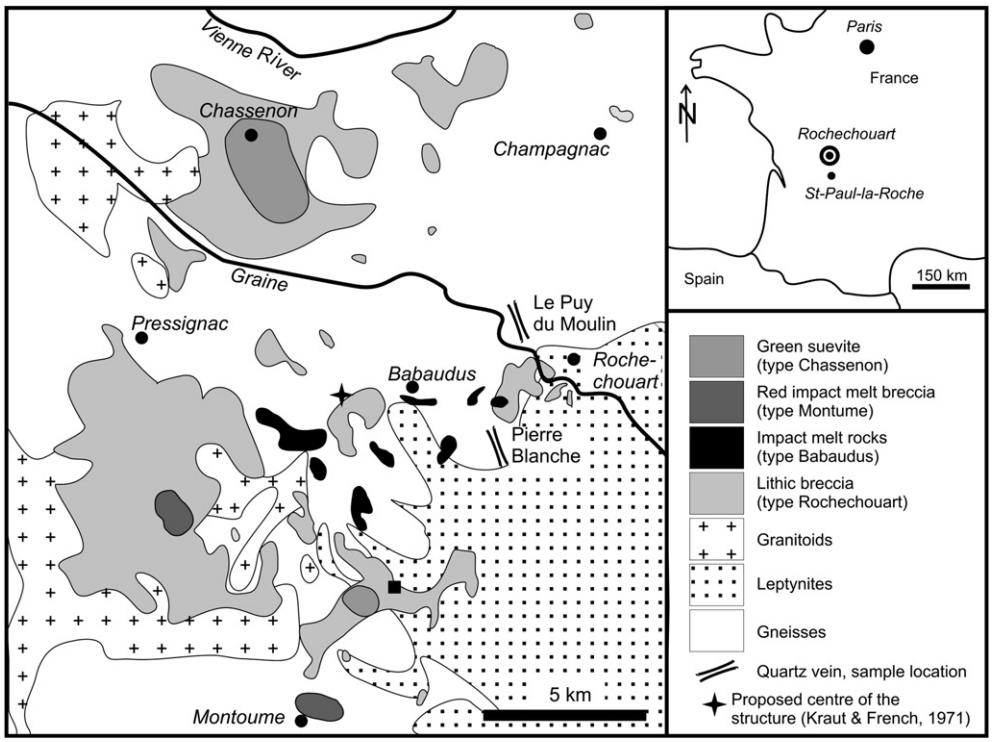

Fig. 1. Simplified geologic map of the Rochechouart impact structure, modified after Kraut and French (1971), Lambert (1977) with the vein quartz locations *Le Puy du Moulin* and *Pierre Blanche* within the impact structure and *St. Paul la Roche* outside the impact structure. Dashed circle indicates probable minimum diameter of the impact structure (~20 km).

2. The Rochechouart impact structure and sample localities

The Rochechouart impact structure, also known as Rochechouart-Chassenon structure, is located in the Western Massif Central, France (Kraut, 1969; Kraut and French, 1971; Lambert, 1977). The structure is eroded; the original crater morphology is not preserved. Based on the distribution of impact breccia and shocked target rocks, however, the diameter is estimated to be 20–25 km (Kraut and French, 1971; Lambert, 1977). The target comprises crystalline basement rocks of the Massif Central. The absence of Triassic and Lower Late Triassic sediments, which form the margin of the Aquitaine Basin 20–25 km W of Rochechouart, indicates that impact took place on a very shallow sea or on shore (Lambert, 1977). This is in accordance with a late Triassic impact age of 214 ± 8 Ma, which is implied by Ar/Ar dating of pseudotachylytes by Kelley and Spray (1997) and by paleomagnetism (Carporzen and Gilder, 2006).

Four different types of impact breccias are distinguished at the Rochechouart structure (Kraut, 1969; Kraut and French, 1971; Lambert, 1977, 1982): 1) Lithic breccias (Rochechouart type); 2) Impact melt rocks (Babaudus type); 3) Red welded melt-matrix breccias (Montume type); 4) Green suevites (melt-fragment breccias, Chassenon type). A system of fractures, shear zones, pseudotachylytes and breccia dikes have been related to various stages of the cratering process (Bischoff and Oskierski, 1987; Kenkmann et al., 2000a; Lambert, 1977; Reimold and Oskierski, 1987).

Shock intensity is higher in the allochthonous breccias compared to the Rochechouart target rocks (Lambert, 1977; Trepmann, 2008). Quartz shock effects in target rock fragments from various impact breccias record high shock pressures of 10–35 GPa by the occurrence of annealed diaplectic glass, mosaicism and various sets of PDFs (Trepmann, 2008). In contrast, quartz in the target rocks contains only rarely one set of rhombohedral PDFs and more commonly basal PDFs, which indicate relatively low shock pressures of <15 GPa and high differential stresses (Trepmann, 2008).

In the gneisses from the Massif Central hydrothermal veins of pure quartz (99% quartz) of several tens of decimetres to several metre thickness are common (Chèvermont et al., 1996; Fig. 1). These hydrothermal quartz veins are associated with pegmatites from the lower and upper gneiss units forming the western edge of the Massif Central (Kraut, 1969; Chèvermont et al., 1996; Désindes et al., 2006). Two locations of quartz veins that are oriented NNW–SSE within the impact structure were sampled at *Le Puy du Moulin* (N45°49.734′–E000°48.770′) and *Pierre Blanche* (N45°48.611′–E000°48.562′) (Fig. 1). The quartz veins are located at a similar distance from the centre of the structure at 5.6 and 5.3 km, respectively. For comparison, the large pure quartz deposit from *St. Paul la Roche* (N45°28′896″–E000°59′692″) at about 40 km to the SE of the centre of the impact structure was sampled (Kraut, 1969; Chèvermont et al., 1996; Désindes et al., 2006, Fig. 1).

3. Methods

Polished thin sections (~30 μm thick) were prepared from the quartz veins. The microstructures were examined in thin section with a polarising microscope, including U-stage measurements of the 3D-orientation of quartz planar features. The crystallographic orientation and microfabric of quartz were analysed by scanning electron microscopy (SEM), using a LEO 1530 instrument with field emission gun, forescatter detector, electron x-ray diffraction (EDX) and electron backscatter diffraction (EBSD) capabilities. The thin sections were chemically polished using a colloidal silica suspension (SYTON®). The SEM was operated at an accelerating voltage of 20 kV, with the thin section tilted at an angle of 70° with respect to the beam, and with a working distance of 25 mm. For the indexing and processing of the data HKL *CHANNEL5* software was used. Transmission electron microscopy (TEM) of the shock effects requires site-specific TEM samples in distinct orientations. Such TEM foils were prepared by the focussed ion beam (FIB) technique

on an FEI Quanta200 3D instrument. Other TEM samples were prepared by conventional ion milling (GATAN PIPS). The TEM samples were examined in a Philips EM301 transmission electron microscope operated at 100 kV. All diffraction contrast images were produced using bright field (BF) conditions. Dislocation densities ρ were estimated from TEM micrographs by counting the number of dislocation lines (N) intersecting a unit area (A) with $\rho = 2\ N/A$ (Karato, 2008).

4. Microfabric of vein quartz within the impact structure

4.1. Pierre Blanche

The quartz veins from *Pierre Blanche*, at a distance of ~5.3 km from the centre of the impact structure, show a heterogeneous microstructure (Fig. 2). Cataclastic zones occur in the partly recrystallized vein quartz (Figs. 2 and 3a, b). The several hundred μm wide cataclastic zones cut through aggregates of recrystallized grains and have relatively sharp boundaries (black arrows in Figs. 2a–c and 3a, b). The cataclastic zones are characterized by a bimodal grain size distribution. Angular clasts have a strongly varying diameter, mostly in the range of 0.05–1 mm, and are surrounded by a fine grained matrix (Figs. 2a–d and 3a, b). Smoothly curved recrystallized grains occur commonly within coarse host crystals in conjugate zones, which are a few grains wide (white arrows in Fig. 2a–c). The recrystallized grain size is relatively uniform, mostly with diameters in the range of 10–50 μm. The recrystallized grains show a close crystallographic relationship to the host quartz (Fig. 3a, c, e, f). In contrast, the cataclastic grains are in a random crystallographic orientation (Fig. 3b, d).

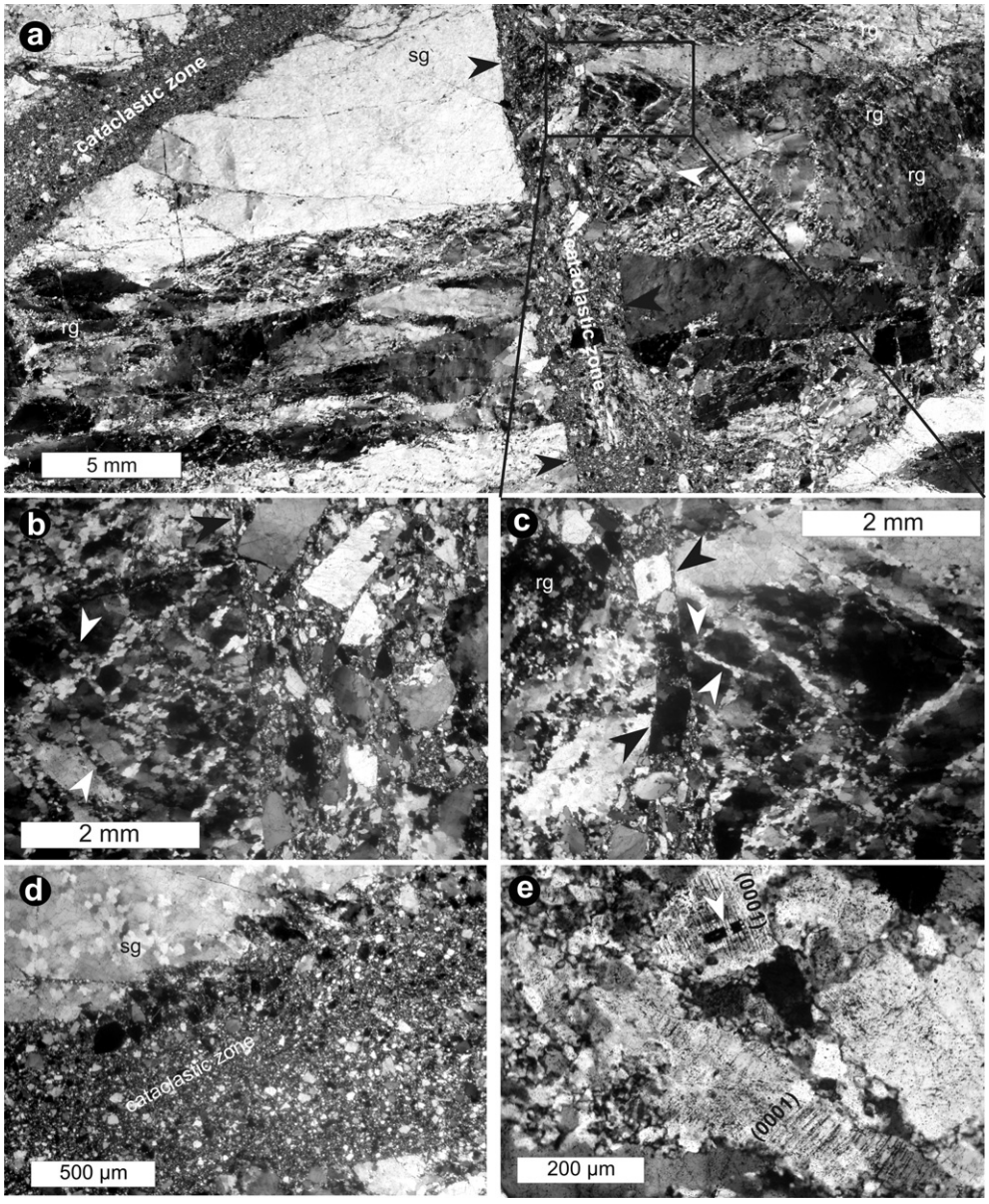

Fig. 2. Optical micrographs taken with crossed polarizers of microstructures in quartz vein from *Pierre Blanche* inside the impact structure. (a) Heterogeneous microstructure (sample Ro69) with large quartz crystals that are partly recrystallized (labelled "rg") and that show subgrains (labelled "sg"). Cataclastic zones cut through the recrystallized grains and have sharp boundaries (black arrows). Location of microstructure presented in (c) is shown by a black rectangle. (b, c) Conjugate zones of recrystallized grains (white arrows) are cut by a cataclastic zone with angular clasts (black arrows). An EBSD map of the microstructure displayed in (c) is presented in Fig. 3. (d) Cataclastic zone occur in a host grain that contains subgrains (labelled "sg", sample Ro69). (e) In larger grains within cataclastic zones (sample Ro68), quartz contains PDFs in the basal plane (0001). FIB-cuts are marked by a white arrow. TEM micrographs from this location are shown in Fig. 4a–d.

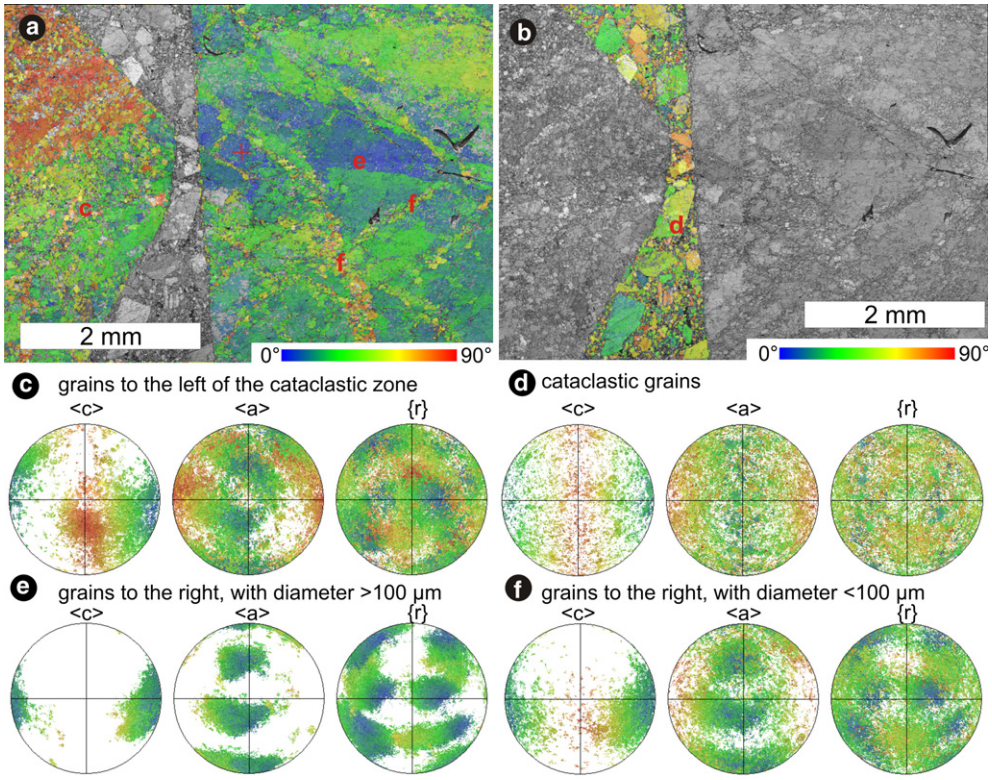

Fig. 3. (a, b) EBSD map (step size 5 μm) of cataclastic zone cutting through partly recrystallized host grain (sample Ro69, *Pierre Blanche*, compare Fig. 2c). EBSD map is displayed by the relative misorientation up to 90° with respect to a reference (red cross) (a) and the cataclastic zone (b). The locations of the areas from which corresponding polefigures are displayed are marked by the respective letters. (c–f) Polefigures of <c>, <a> axes and poles to {r} planes of the host grain to the left of the cataclastic zone (c), cataclastic grains (d), grains to the right of cataclastic zone with diameter >100 μm (e) and the recrystallized grains <100 μm (f), in colours corresponding to the map in (a and b, respectively). (For interpretation of the references to colour in this figure legend, the reader is referred to the web version of this article.)

Quartz in cataclastic zones contains planar deformation features (PDFs) parallel to the (0001) basal plane (Fig. 2e). TEM reveals that the basal PDFs represent mechanical Brazil twins in the (0001) plane (Fig. 4a–d). The Brazil twins show a complex crosscutting relationship with low angle grain boundaries (LAGBs, black arrows in Fig. 4a–d). Straight defects occur at an angle to the basal PDFs and are interpreted to represent healed microcracks (white arrows in Fig. 4c, d). Straight LAGBs occur also in grains that do not show basal PDFs (white arrows in Fig. 4e, f). Fluid inclusions are common (Fig. 4e, f). LAGBs can be sutured (Fig. 4g) and small recrystallized grains with a low defect density occur (Fig. 4h).

4.2. *Le Puy du Moulin*

At *Le Puy du Moulin*, located ~5.6 km from the centre of the impact structure, vein quartz shows narrow cataclastic zones within large host grains that show conspicuous undulating deformation lamellae and wavy LAGBs (Fig. 5a, b). The undulating deformation lamellae are not in a preferred crystallographic orientation. Across these lamellae the relative misorientation is below 2°. The host grain shows generally an internal relative misorientation of smaller than 15° (Fig. 5c, e). The angular cataclastic grains have a quasi-random crystallographic orientation (Fig. 5d, f).

5. Microfabric of vein quartz outside the impact structure

The vein quartz from *St. Paul la Roche* ~40 km SE outside the impact structure is coarse grained. Commonly, a thin section covers one single crystal (Fig. 6). Nevertheless, it shows a heterogeneous microstructure with a prevalent system of healed microcracks (black arrows in Fig. 6a–c, e, f), LAGBs and undulatory extinction (Fig. 6b–d). Trépied et al. (1980) documented that the "cleaved" quartz from *St. Paul la Roche* exhibits straight features preferentially oriented parallel to the ***r*** rhombohedral planes (Fig. 6c). Healed microcracks observed in this study are commonly subbasal or parallel to the ***r*** rhombohedra (Fig. 6). Wavy LAGBs follow these healed microcracks bounding irregular domains with relative misorientations below 20° (Figs. 6b, c and 7). Along the healed microcracks, aggregates of subgrains occur, which show a slightly higher relative misorientation of up to 20° and Dauphiné twin orientations occur (Figs. 6e and 8). Single recrystallized grains decorate healed fractures (Figs. 6f and 9). They make up less than 5% of the vein quartz and have a diameter mostly in the range of 10–100 μm. The shape of the recrystallized grains can be isometric or elongate with the long axis of the grains parallel to the fracture. They occur in random crystallographic orientation and with no systematic crystallographic relationship to the host grain (Fig. 9a, c). The misorientation of the recrystallized grains to the host grain is 30°–90° (Fig. 9a). Subgrains similar in shape and size with misorientations of 5°–8° to the host grain occur together with these recrystallized grains (Fig. 9a). Deformation bands, across which a relative misorientation of 2°–10° is revealed, are commonly parallel to prism planes (Figs. 6b, 7a and 10a, c). They show highly variable widths in the range of 10–100 μm, an irregular, large spacing.

The most conspicuous features, however, are undulating deformation lamellae that are very similar to those in the vein quartz from *Le Puy du Moulin* (compare Figs. 5a, b and 6c, d). They obviously do not follow crystallographic planes and do not show a crystallographic preferred orientation. The relative misorientation of the different domains defined by the lamellae is generally below 2° (Fig. 10). The width of the lamellae detectable by EBSD is mostly in the range of 5–30 μm and corresponds to their spacing. There

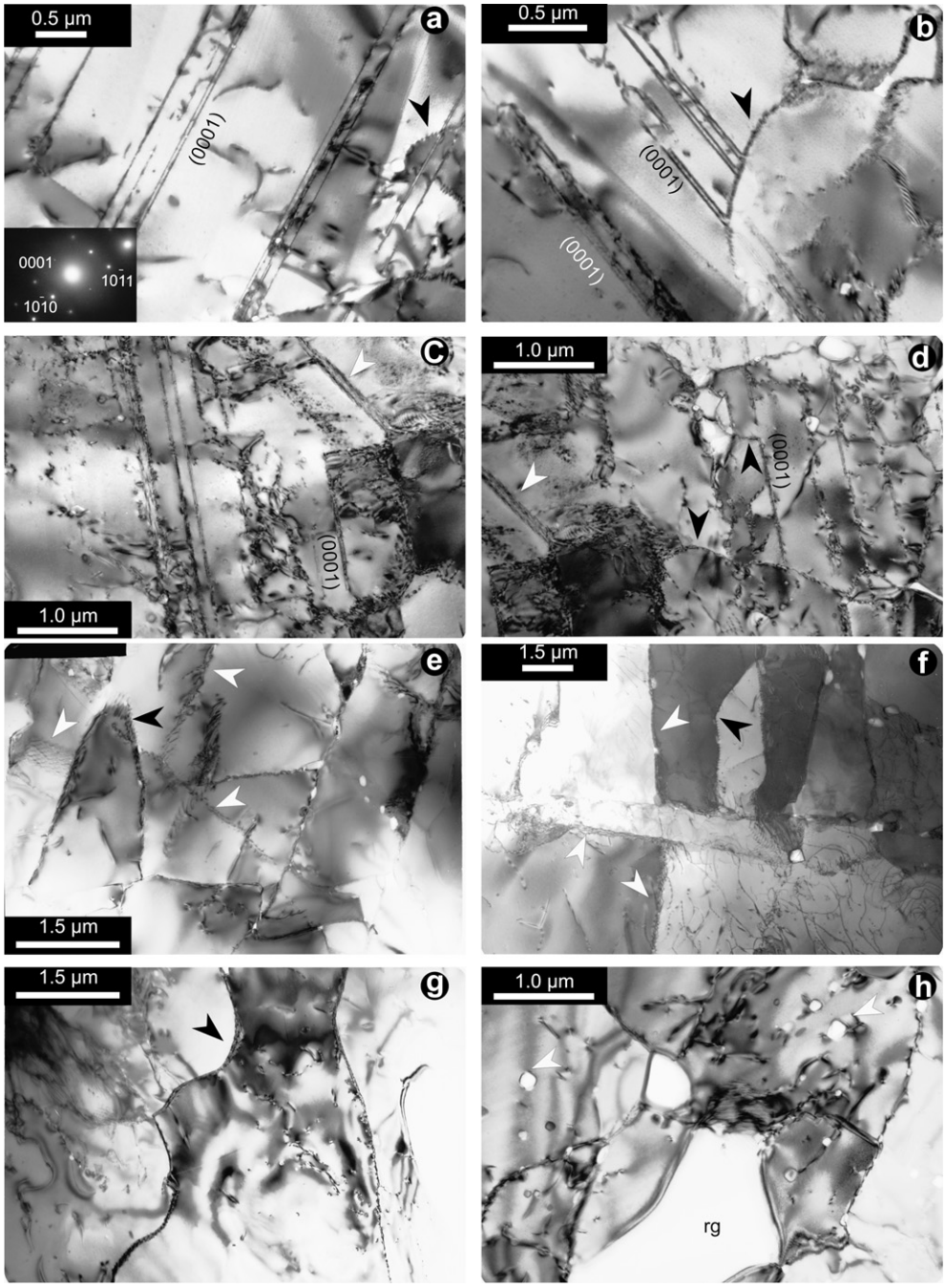

Fig. 4. TEM bright field micrographs of vein quartz from *Pierre Blanche* (sample Ro68). (a–d) Complex crosscutting relationship of straight Brazil twin boundaries in the basal plane (0001) with curved LAGBs (black arrows) and straight defects that are interpreted to represent healed microcracks (white arrows; FIB-prepared samples, location of a FIB-cut is shown in Fig. 2e). (e–h) TEM foils are prepared by conventional ion milling. (e, f) The crystal is disintegrated by various straight (white arrows) and curved (black arrows) LAGBs. (g) LAGBs can be sutured, indicating migration (black arrow). (h) Tiny new grains devoid of defects are labelled "rg" and fluid inclusions are marked by white arrows.

appears to be a proportional dependence between width and misorientation. Undulating deformation lamellae with a relative misorientation below 1° reveal a width of ~5 µm (Fig. 10a, b). If the relative misorientation up to 2°, the width of the lamellae is up to 30 µm (Fig. 10e–h). In TEM, samples that show optically fine undulating deformation lamellae (Figs. 6c, d and 10a–d), diffuse dislocation walls or poorly ordered LAGBs (arrows in Fig. 11a–c) confine domains of about 1 µm width with different diffraction conditions, where dislocations are in or out of contrast at slightly different tilting positions. The dislocations are straight or curved and the density is on the order of 10^{13} m^{-2} (Fig. 11a–d). In samples showing broader undulating deformation lamellae (Figs. 6b and 10e–h), well-ordered LAGBs and fluid inclusions are common (Fig. 11e–h). Dauphiné twin boundaries occur next to LAGBs (Fig. 11e).

6. Discussion

6.1. Shock effects

Basal PDFs that represent mechanical Brazil twins in the (0001) plane occur in the vein quartz from *Pierre Blanche* (Figs. 2d, e and 4a–d). These features are uniquely characteristic of shock during

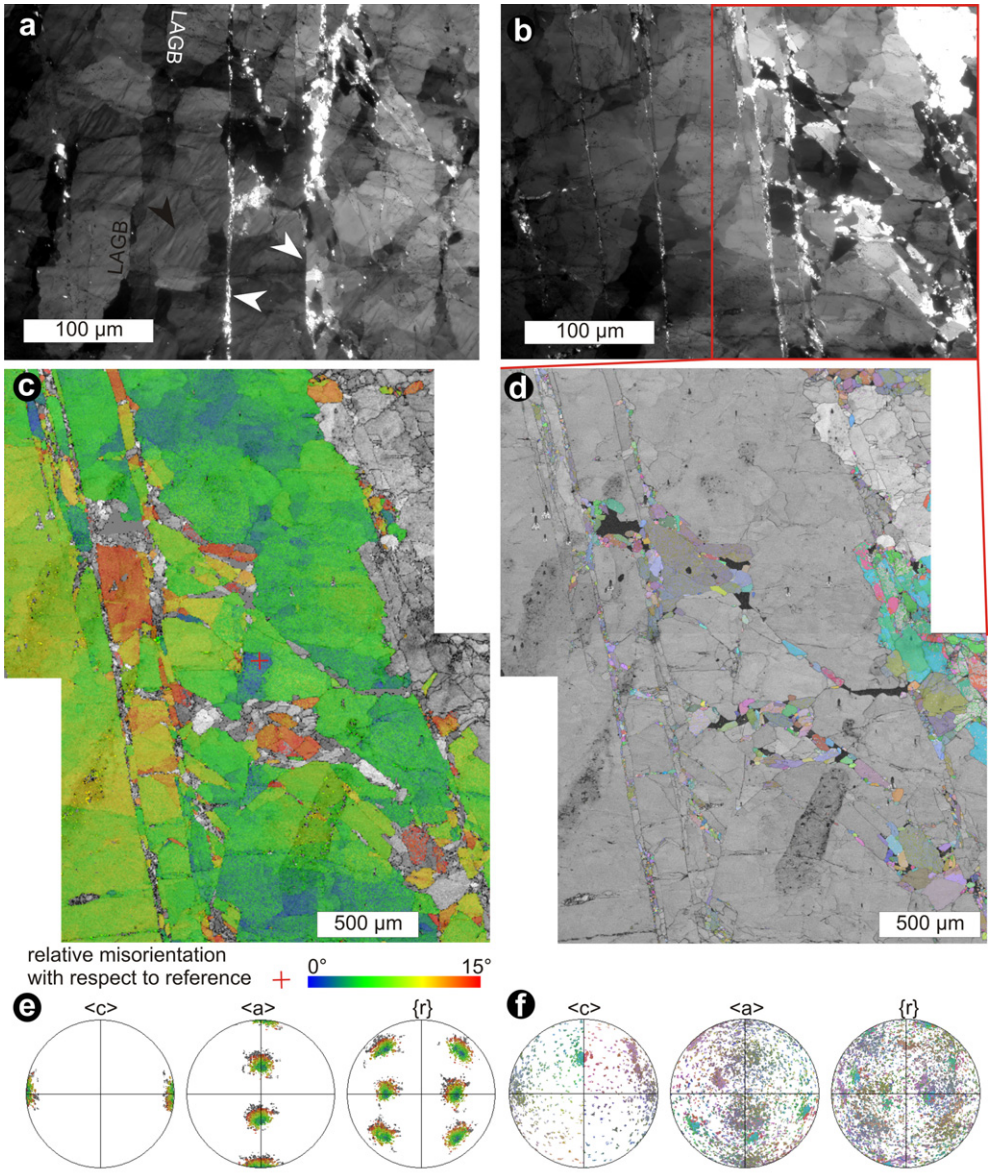

Fig. 5. Microstructure in quartz vein from *Le Puy du Moulin* (sample Ro123). (a, b) Optical micrographs (crossed polarizers) showing LAGBs forming wavy bands, undulating deformation lamellae (black arrow) and narrow cataclastic zones (white arrows). (c, d) EBSD map (step size 2.5 µm) of the microstructure marked by the red rectangle shown in (b). The map in (c) is displaying the relative misorientation of up to 15° with respect to a reference (red cross). The map in (d) shows the different crystallographic orientation of cataclastic grains by different colours. (e) Polefigures of <c>, <a> axes and poles to {r} planes in colours corresponding to the map in (c). (f) Polefigures of <c>, <a> axes and poles to {r} planes in colours corresponding to the map in (d). (For interpretation of the references to colour in this figure legend, the reader is referred to the web version of this article.)

meteorite impact cratering (e.g., Goltrant et al., 1992; Leroux et al., 1994; Leroux and Doukhan, 1996). PDFs parallel to rhombohedral planes that are assumed to develop by a localized transformation of quartz into a high-density amorphous phase (e.g., Goltrant et al., 1992; Langenhorst, 1994) do not occur in the described vein quartz. The occurrence of PDFs in different crystallographic orientations has been found to depend on the shock pressure (Robertson, 1975; Martini, 1991; Gratz et al., 1992; Langenhorst, 1994; Stöffler and Langenhorst, 1994; Langenhorst and Deutsch, 1994; Grieve et al., 1996). Based on the comparison of shock-experiments and the occurrence in naturally shocked quartz, the absence of rhombohedral PDFs and the occurrence of basal PDFs imply relatively low shock pressures $<c.$ 8 GPa (Robertson, 1975; Stöffler and Langenhorst, 1994; Grieve et al., 1996; French, 1998). Mechanical Brazil twins indicate a high shock-induced differential stress on the order of a few GPa (McLaren et al., 1967; Leroux et al., 1994; Leroux and Doukhan, 1996; Trepmann and Spray, 2005, 2006; Trepmann, 2008).

Cataclastic zones are characteristic microstructures in quartz veins within the Rochechouart impact structure and do not occur in quartz veins from *St. Paul la Roche* outside the impact structure. Cataclastic deformation can result from both, tectonic deformation and impact cratering. The observation, however, that basal PDFs are restricted to the cataclastic zones implies that they formed concomitant and therefore the cataclastic zones are interpreted to be shock-induced. This is consistent with the observation that the cataclastic zones cut through the crystal-plastic deformation features (Figs. 2a–c and 3a, b). The straight defects observed by TEM that can occur together or independently from basal PDFs (Fig. 4c–f) are interpreted as submicroscopic expressions of cataclastic deformation.

Although the distance of the quartz veins at *Le Puy du Moulin* from the centre of the Rochechouart impact structure is 5.6 km versus 5.3 km for the quartz veins at *Pierre Blanche*, the shock intensities recorded by the microstructure (Table 1) are very

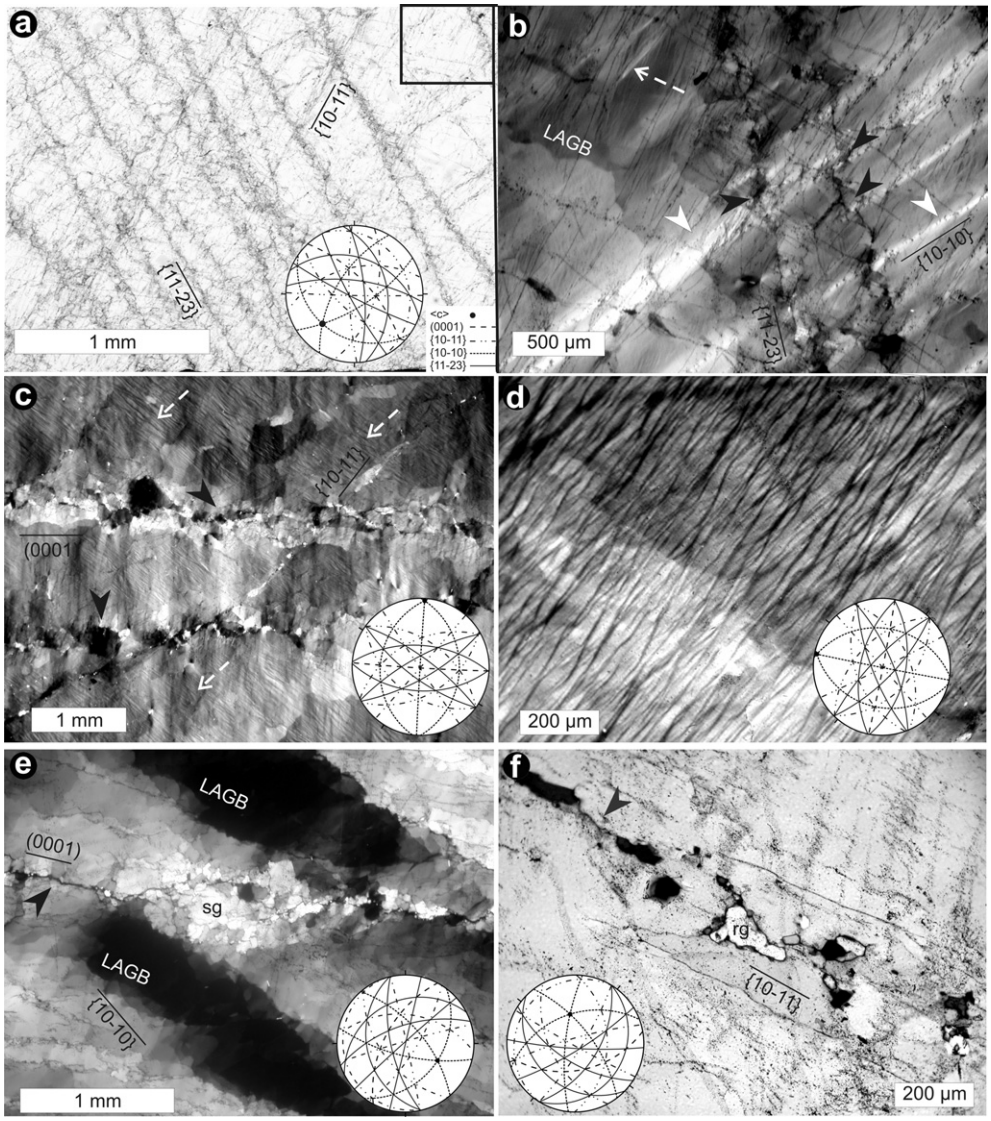

Fig. 6. Photomicrographs (crossed polarizers) of vein quartz from *St. Paul la Roche* outside the impact structure. The crystallographic orientation of the displayed crystal is shown in the stereographic projections of the lower hemisphere, the legend for all projections is given in (a). (a) System of healed microcracks (black arrows, sample Ro105). The location of the microstructure presented in (b) is shown by a black rectangle. (b) Irregular healed microcracks (black arrows) occur at an angle to wavy LAGBs. Deformation bands (white arrows) apparently offset the microcracks in different directions (black arrows). Undulating deformation lamellae are marked by white, dashed arrows. An EBSD map of the microstructure is presented in Fig. 7. (c) Overview of microstructure showing prevalent undulating deformation lamellae (white, dashed arrows), healed microcracks (black arrows) and a deformation band (white arrow, sample Ro102). (d) Close up of undulating deformation lamellae (sample Ro102). (e) Aggregate of subgrains is aligned along a fracture. An EBSD map of this microstructure is presented in Fig. 8 (sample Ro108). (f) Recrystallized grains are aligned along a fracture. An EBSD map of this microstructure is presented in Fig. 9 (sample Ro108).

different. This may be caused by (1) heterogeneities of the target, as grain boundaries, lithological interfaces, porosity and open fissures influence the complex interaction of shock wave and target (e.g., Kieffer et al., 1976; Kenkmann et al., 2000b; Heider and Kenkmann, 2003) and/or (2) a primary uneven distribution of the shock intensities, e.g., oblique impacts can lead to a non-circular distribution of shock effect (e.g., Pierazzo and Melosh, 2000).

6.2. The "starting material": pre-shock deformation

6.2.1. Microcracking, crystal-plastic deformation and recrystallization

At *St. Paul la Roche*, the microfabric of quartz veins does not indicate shock wave-induced deformation or transformation at a dynamic high hydrostatic pressure. The "cleaved" quartz (Trépied et al., 1980) documents crystallographically controlled microcracking commonly along the basal plane and ***r*** rhombohedral planes. These microcracks are clearly distinctive from the closely spaced, narrow and strictly planar rhombohedral (mostly ***π***, ***w*** rhombohedra) or basal PDFs, which are well known shock effects in quartz (e.g., Goltrant et al., 1992; Langenhorst, 1994; Leroux et al., 1994; Leroux and Doukhan, 1996) and which occur in the impactites of the Rochechouart impact structure (Trepmann, 2008). Furthermore, crystal-plastic deformation is evident from deformation bands, undulating deformation lamellae, subgrains and recrystallized grains. Similar microstructures occur as well in the vein quartz at *Le Puy du Moulin* within the impact structure (compare Figs. 5a, b and 6b, and EBSD maps displayed in Figs. 5 and 7). The undulating deformation lamellae observed in quartz

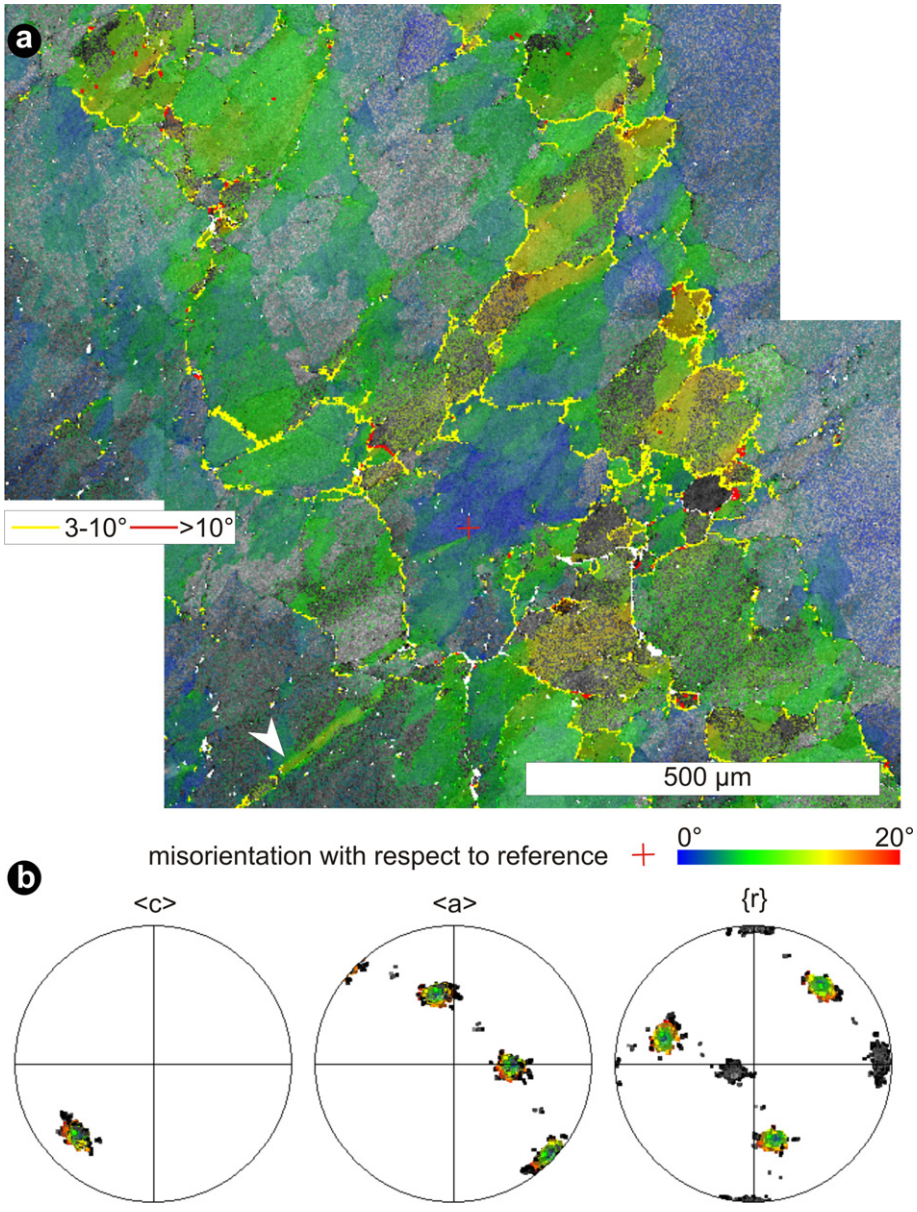

Fig. 7. (a) EBSD map (step size 1 µm) of vein quartz with wavy LAGBs along healed microcracks from *St. Paul la Roche* (compare Fig. 6b, sample Ro105), displaying the relative misorientation up to 20° with respect to a reference (red cross). Yellow lines represent LAGBs with relative misorientations of 3–10° and red lines high angle grain boundaries with misorientations >10°. White arrow is pointing to a deformation band. (b) Polefigures of <c>, <a> axes and poles to {r} planes in colours corresponding to the map in (a). (For interpretation of the references to colour in this figure legend, the reader is referred to the web version of this article.)

veins within and outside the impact structure do not show a crystallographic preferred orientation. This is in contrast to subbasal deformation lamellae common in tectonically deformed quartz, also known as Böhm lamellae, which are revealed by TEM to be associated with curved dislocation walls or poorly ordered LAGBs defining elongate subgrains of irregular shape (e.g., McLaren et al., 1970; Avé Lallement and Carter, 1971; McLaren and Hobbs, 1972; Christie and Ardell, 1974; White, 1973, 1975; Drury, 1993; Trepmann and Stöckhert, 2003). The undulating deformation lamellae occur in a fine spacing and are prevalent throughout a complete thin section (Figs. 6c, d and 10a, sample Ro102). In TEM, these features are represented by domains of about 1 µm width with a high dislocation density on the order of 10^{13} m^{-2} and that are confined by irregular dislocation walls and LAGBs (Fig. 11a–d). In other samples, undulating lamellae are broader with a higher and more irregular spacing and show a slightly higher misorientation (Figs. 6b and 10e, f, sample Ro105). It is suggested that the difference in the appearance is the degree of recovery, whereby the finer undulating deformation lamellae represent a lower degree and the broader represent the higher degree of recovery. The undulating deformation lamellae are thought to represent a modified microstructure. The original microstructure was characterized by a homogeneously distributed high dislocation density. Due to recovery, dislocations of opposite sign are eliminated and geometrically necessary dislocations are progressively arranged into dislocation tangles, walls, arrays and LAGBs. The dislocation walls (Fig. 11a–d) from sample Ro102 represented by prevalent and fine deformation lamellae (Figs. 6c, d and 10a) experienced less modification by recovery compared to sample Ro105. The latter show broader deformation lamellae

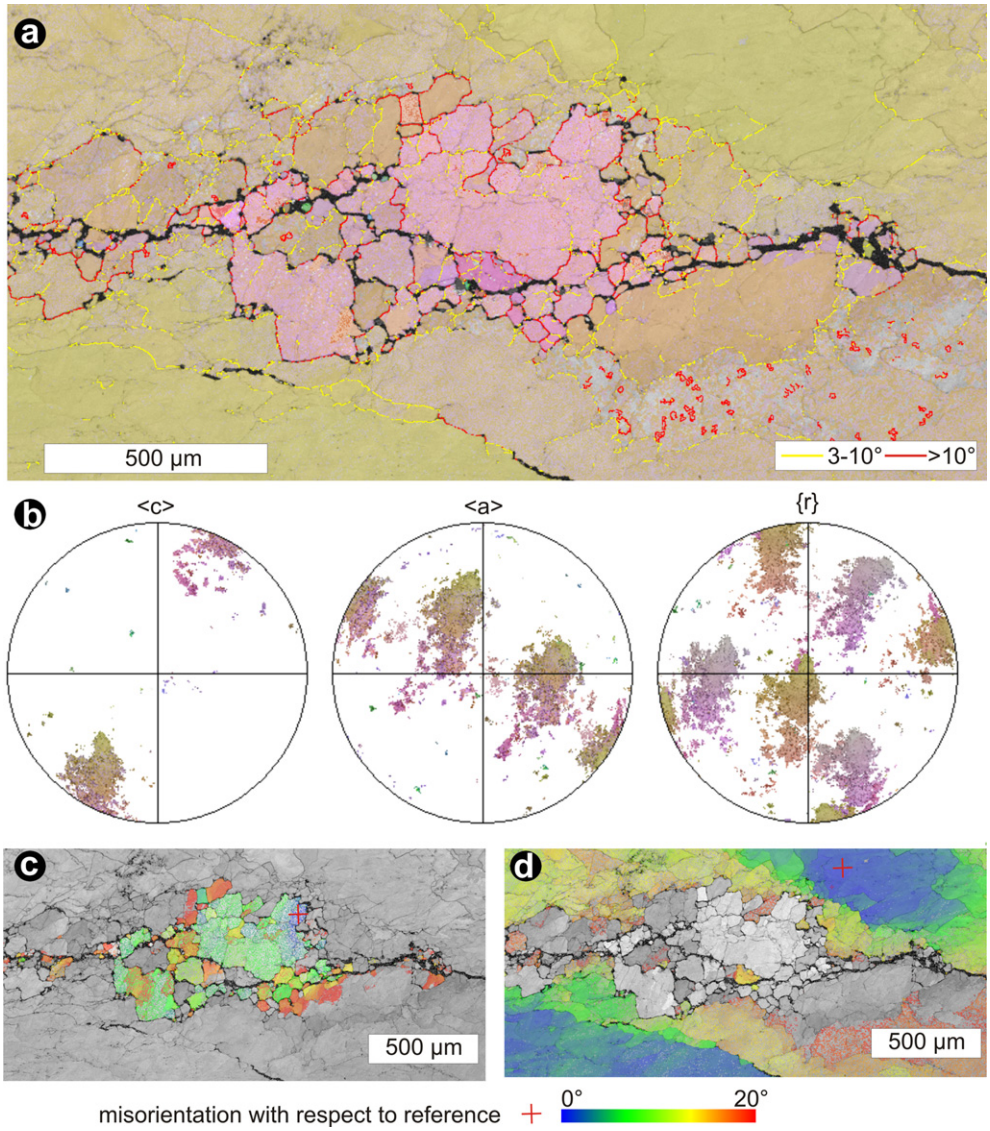

Fig. 8. (a) EBSD map (step size 2 µm) of subgrains along a fracture in vein quartz from *St. Paul la Roche* outside the impact structure (compare Fig. 6e, sample Ro108), displaying the crystallographic orientation by different colours. Yellow lines represent LAGBs with relative misorientations of 3–10° and red lines high angle grain boundaries with misorientations >10°. (b) Polefigures of <c>, <a> axes and poles to {r} planes in colours corresponding to the map in (a). (c, d) EBSD map is displaying the relative misorientation up to 20° of the recrystallized and the host quartz grain, respectively. (For interpretation of the references to colour in this figure legend, the reader is referred to the web version of this article.)

(Fig. 6b) and the TEM microstructure is characterized by a lower dislocation density (Fig. 11e, h) and well-ordered LAGBs (Fig. 11d, g). The undulating deformation lamellae would in this way reflect a "left over-microstructure" representing a stage of dislocation production at high stress with restricted dynamic recovery. Strain hardening probably caused microfracturing, as indicated by the healed microcracks. The well-ordered LAGBs, curved dislocations and dislocation loops (Fig. 11e–h), indicate a stage of subsequent dislocation climb and recovery. Recrystallized grains are rare in quartz veins from *Le Puy du Moulin* inside the impact structure and *St. Paul la Roche* outside the impact structure and are localized aligned along healed fractures (Figs. 6f and 9). The recrystallized grains do not show a substructure. This, and their random crystallographic orientation, as well as the absent crystallographic relationship to the host grain, indicate localized quasi-static recrystallization (Fig. 9).

At *Pierre Blanche* inside the impact structure, quartz veins are largely recrystallized. The recrystallized grains are smoothly curved and show a close crystallographic relationship to the host quartz (Fig. 3f) and indicate dynamic recrystallization (e.g., White, 1973; Poirier, 1985). The recrystallized grains occur in conjugate zones (Fig. 2b, c), which represent initial highly damaged semi-brittle zones generated during a preceding high stress event. Along these zones, deformation and recrystallization processes occur localized during attenuating stresses.

In summary, the quartz veins of *St. Paul la Roche*, *Pierre Blanche* and *Le Puy du Moulin* record two stages of crystal-plastic deformation/recrystallization (Table 1): (1) An initial stage of high stress deformation with glide-controlled deformation and microcracking. (2) At lower stresses, dislocation climb and recovery allowed the generation of deformation bands and wavy LAGBs. At localized sites of enhanced strain during the high stress event, dynamic recrystallization occurred in the vein quartz at *Pierre Blanche*. Quasi-static recrystallization occurred by growth of randomly oriented quartz grains in the quartz veins at *St. Paul la Roche* and *Le Puy du Moulin*.

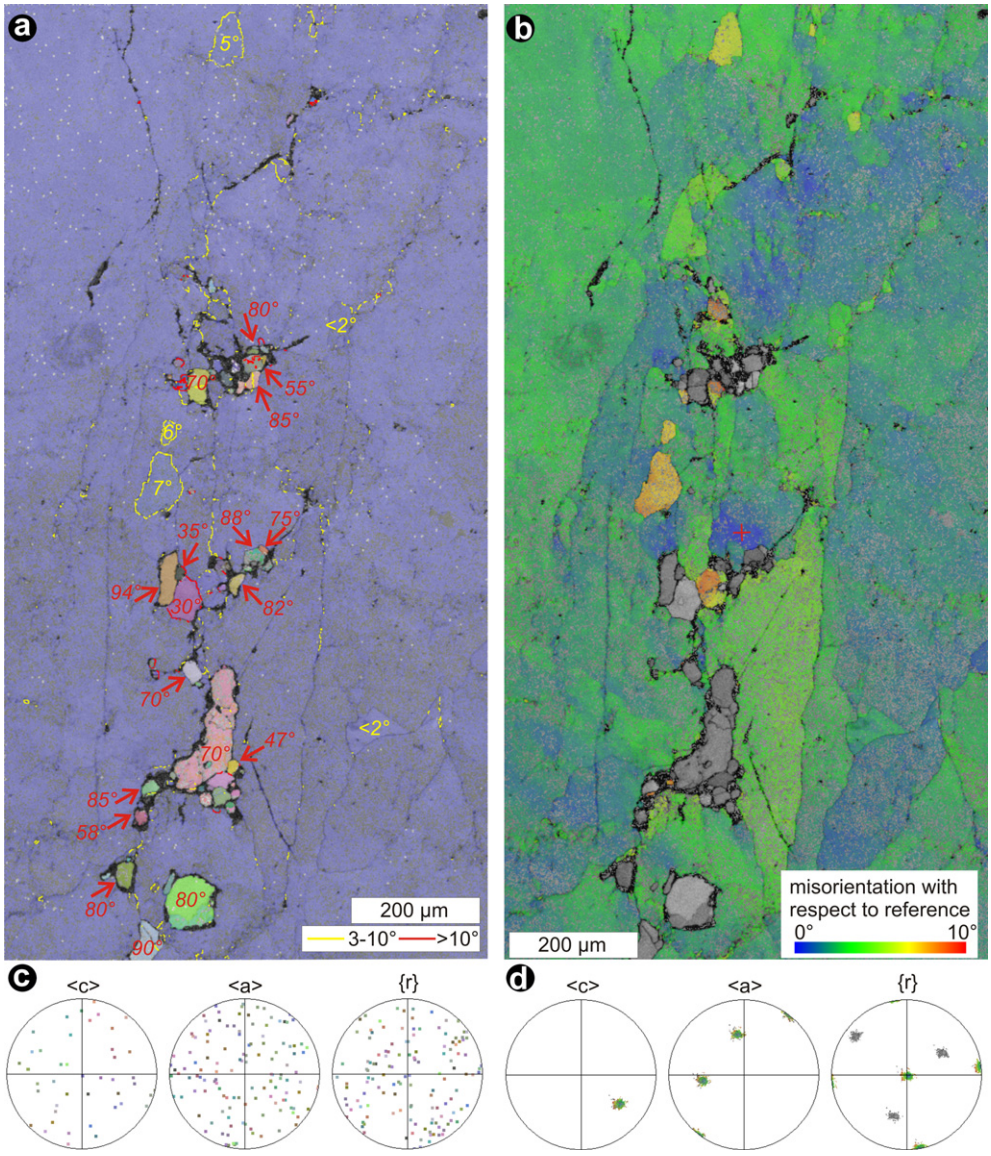

Fig. 9. (a) EBSD map (step size 1.5 µm) of recrystallized grains aligned along fractures in vein quartz from *St. Paul la Roche* outside the impact structure (compare Fig. 6f, sample Ro108), displaying the crystallographic orientation by different colours. Yellow lines represent LAGBs with misorientations of 3–10° and red lines high angle grain boundaries with misorientations >10°. The numbers in red are misorientation angles of recrystallized grains with respect to the host grain. (b) EBSD map is displaying the relative misorientation of the host quartz grain by different colours. (c, d) Polefigures of <c>, <a> axes and poles to {r} planes in colours corresponding to the maps in (a) and (b), respectively. (For interpretation of the references to colour in this figure legend, the reader is referred to the web version of this article.)

6.2.2. Temperature

Quartz microfabrics have been used as empirical indicators of temperature and the thermal history in correlation with petrologic thermobarometers or thermochronometric data (e.g., Voll, 1976; Dunlap et al., 1997; Dresen et al., 1997; Stöckhert et al., 1999; Stöckhert and Duyster, 1999; Brix et al., 2002; Hirth et al., 2001; Stipp et al., 2002a,b). These observations on natural rocks suggest that temperatures of at least 250–300 °C are required for the effective recovery and recrystallization of quartz. In annealing experiments, Trépied et al. (1980) described a marked modification of the microstructures in the *St. Paul la Roche* quartz with a decreased dislocation density and an increase in well-ordered LAGBs after annealing at 800 °C for 3 days. Given the indication of only restricted modification by recovery and recrystallization and the high free dislocation density in the *St. Paul la Roche* quartz, the temperatures for the crystal-plastic deformation are supposed to be not much higher than the minimum temperature for crystal plasticity of quartz and therefore assumed to be in the range of 300 ± 50 °C.

6.2.3. Geological implication

The undulating deformation lamellae, representing domains of high dislocation density indicate a stage of glide-controlled deformation with a high rate of dislocation production (Table 1). Shock wave-induced stresses and strain rates are generally assumed to be too high and the shock duration of several seconds at the most (depending on the size of the projectile) too low to cause major crystal-plastic deformation except for mechanical twinning (Gratz et al., 1992; Langenhorst, 1994; Grieve et al., 1996). Effective recrystallization and recovery require concomitant or preceding crystal-plastic deformation. Furthermore, the observed crosscutting relations (Figs. 2 and 3) indicate that crystal-plastic deformation and

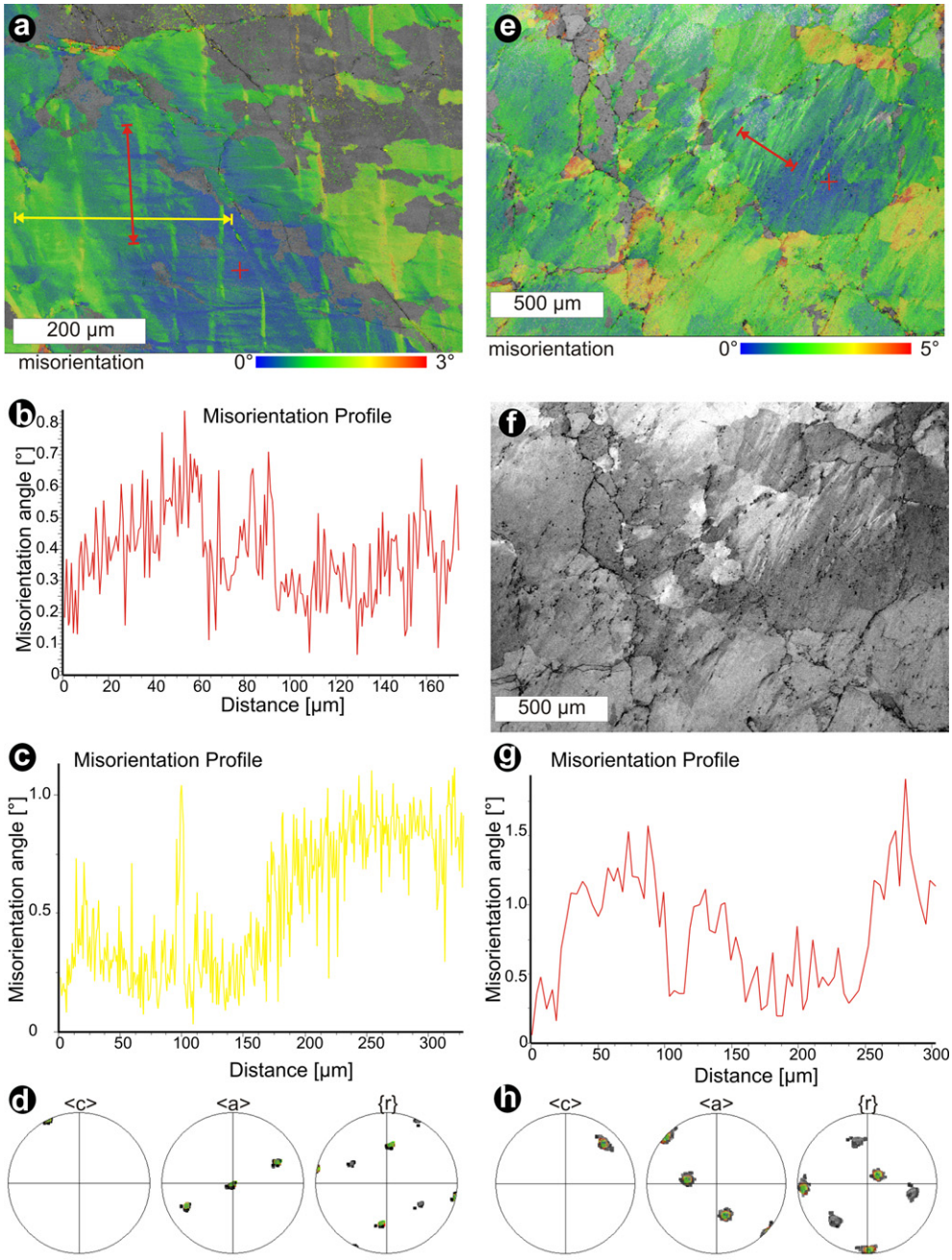

Fig. 10. (a) EBSD map (step size 0.8 µm) of vein quartz with deformation lamellae (compare Fig. 6c, d) from *St. Paul la Roche* (sample Ro102), displaying the relative misorientation with respect to a reference (red cross). The red line is indicating the misorientation profile shown in (b). The yellow line is indicating the misorientation profile shown in (c). (b) Misorientation profile from red line shown in (a). (c) Misorientation profile from yellow line shown in (a). (d) Polefigures of <c>, <a> axes and poles to {r} planes in colours corresponding to the map in (a). (e) EBSD map (step size 3 µm) of vein quartz with deformation lamellae (compare Fig. 6b) from *St. Paul la Roche* (sample Ro105), displaying the relative misorientation with respect to a reference (red cross). The red line is indicating the misorientation profile shown in (g). (f) EBSD map displaying pattern quality (band contrast). (g) Misorientation profile from line shown in (e). (h) Polefigures of <c>, <a> axes and poles to {r} planes in colours corresponding to the map in (e). (For interpretation of the references to colour in this figure legend, the reader is referred to the web version of this article.)

recrystallization pre-date the shock effects. Thus, the crystal-plastic deformation and subsequent recrystallization recorded by the vein quartz are interpreted to be pre-shock features.

A microfabric development with initial crystal-plastic deformation at high stress accompanied by microcracking and subsequent recrystallization at low stress and at temperatures in the range of 300 ± 50 °C is characteristic for episodic deformation at mid-crustal conditions caused by stress redistribution related to seismic faulting in the overlying upper crust (Trepmann and Stöckhert, 2003; Nüchter and Stöckhert, 2008). Furthermore, localized quasi-static recrystallized grains along microcracks, very similar to those observed from the quartz veins at *St. Paul la Roche*, have been produced in laboratory experiments, in which inhomogeneous deformation at high stress was followed by static annealing to simulate the natural stress history in the middle crust during the seismic cycle (Trepmann et al., 2007). Thus, the pre-shock deformation features in the hydrothermal quartz veins are proposed to result from coseismic loading and postseismic stress relaxation below the seismogenic layer. The microstructure at *Pierre Blanche* would imply a higher accumulation of strain

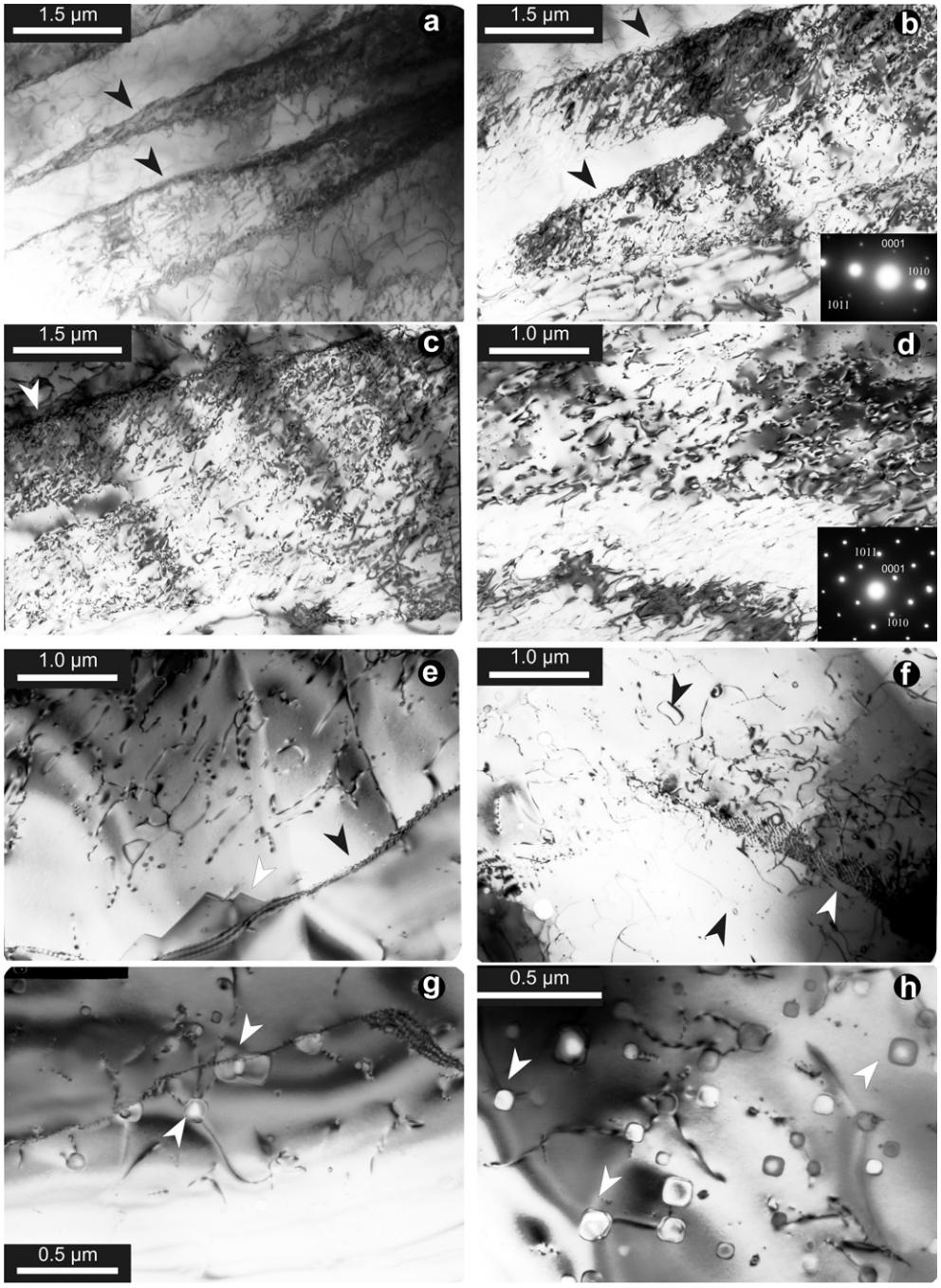

Fig. 11. TEM bright field micrographs of vein quartz from *Pierre Blanche*. TEM foils are prepared by ion milling (a–e sample Ro102, f–h sample Ro105). Optically all samples show undulating deformation lamellae (a–e compare Figs. 6c, d and 10a, f–h sample compare Figs. 6b and 10e). (a–d) Dislocation walls or poorly ordered LAGBs (arrows) confine domains with a width of about 1 µm, where dislocations are in or out of contrast at slightly different tilting conditions. The dislocation density is on the order of 10^{13} m^2. (e) Well-ordered LAGBs (black arrow) occur. The white arrow is pointing at typically zig-zag-shape Dauphiné twin boundaries. (f) Dislocations are bent and loops are frequent (black arrow). The white arrow is pointing at an LAGB. (g, h) Fluid inclusions are common (white arrows).

Table 1
Compilation of the microstructures characteristic of the various deformation stages.

Sample location	Distance to assumed centre of the impact structure	Pre-shock deformation		Shock-induced deformation
		High stress glide-controlled deformation accompanied by microcracking	Low stress recovery and recrystallization	
St. Paul la Roche	40 km SE (outside the impact structure)	deformation lamellae, microcracks	localized subgrains, static recrystallized grains	
Le Puy du Moulin	5.6 km, (within the impact structure)	deformation lamellae, microcracks	localized subgrains	cataclastic zones
Pierre Blanche	5.3 km (within the impact structure)	deformation lamellae, microcracks	subgrains, conjugate zones of dynamically recrystallized grains	cataclastic zones mechanical Brazil twins (basal PDFs)

during stress relaxation compared to *St. Paul la Roche* and *Le Puy du Moulin*. Such local variations on the relative rates of recrystallization and stress relaxation on small distances are characteristic for short-term episodic deformation (Trepmann and Stöckhert, 2003).

7. Summary and conclusions

Quartz veins from the Rochechouart impact structure show a complex microfabric that is strongly influenced by pre-shock crystal-plastic deformation and shock-related cataclastic deformation (Table 1). Pre-shock microstructures are conjugate zones of recrystallized grains, LAGBs and undulating deformation lamellae. Similar microstructures are also found in hydrothermal quartz veins from the Western Massif Central at *St. Paul la Roche*, about 40 km to the SE of the centre of the impact structure. No shock effects occur in these quartz veins. The undulating deformation lamellae do not show a preferred crystallographic orientation. In the TEM, they represent domains of about 1 μm width with a high density of dislocations and that are confined by dislocation walls or poorly ordered LAGBs. These microstructures give evidence of an initial stage of high stress with a high rate of dislocation production by glide-controlled deformation. This was probably accompanied by microcracking, as indicated by healed fractures (*St. Paul la Roche* and *Le Puy du Moulin*) or conjugate zones of recrystallized grains (*Pierre Blanche*). Subsequently, quasi-static recovery and restricted recrystallization (*St. Paul la Roche* and *Le Puy du Moulin*), or intense dynamic recrystallization (*Pierre Blanche*) occurred at attenuated stresses. The pre-shock crystal-plastic deformation probably took place at temperatures of 300 ± 50 °C. Such a microfabric development with initial high stress glide-controlled deformation accompanied by microcracking and subsequent modification by recovery and recrystallization at low stress is characteristic for coseismic loading and postseismic stress relaxation in the middle crust below the seismogenic layer.

At the Rochechouart impact structure (*Pierre Blanche* and *Le Puy du Moulin*), these pre-shock microstructures are overprinted by intense cataclastic deformation related to the late Triassic meteorite impact. Cataclastic zones cut through pre-shock microstructures. Restricted to the cataclastic zones, basal PDFs that represent mechanical Brazil twins occur. These shock effects indicate differential stresses on the order of a few GPa. As no rhombohedral PDFs occur, a low shock pressure of $<c.$ 8 GPa is indicated.

Both, pre-shock deformation and shock-induced deformation indicated by the microfabric in quartz veins from the Rochechouart impact structure are short-term processes far from equilibrium. Nevertheless, shock-induced deformation involves extreme loading rates, inhibiting effective crystal-plastic processes apart from mechanical twinning and localized dislocation glide.

Acknowledgements

Financial support by the Deutsche Forschungsgemeinschaft within the scope of the Collaborative Research Centre 526 "Rheology of the Earth – from the upper crust into the subduction Zone" is gratefully acknowledged. John Spray and Thomas Kenkmann are thanked for constructive reviews.

References

Avé Lallement, H.G., Carter, N.L., 1971. Pressure dependence of quartz deformation lamellae orientations. American Journal of Science 270, 218–235.

Bischoff, L., Oskierski, W., 1987. Fractures, pseudotachylite veins and breccia dikes in the crater floor of the Rochechouart impact structure, SW-France, as indicators of crater forming processes. In: Pohl, J. (Ed.), Research in Terrestrial Impact Structures. Friedr Vieweg and Sohn, Braunschweig/Wiesbaden, pp. 5–29.

Brix, M.R., Stökhert, B., Seidel, E., Theye, T., Thomson, S.N., Küster, M., 2002. Thermobarometric data from a fossil zircon partial annealing zone in high pressure – low temperature rocks of eastern Crete, Greece. Tectonophysics 349, 309–326.

Carporzen, L., Gilder, S.A., 2006. Evidence for coeval Late Triassic terrestrial impacts from the Rochechouart (France) meteorite crater. Geophysical Research Letters 33, L19308. doi:10.1029/2006GL027356.

Chèvermont, P., Floch′, H.J.P., Ménillet, F., Stussi, J.M., Delbos, R., Sauret, B., Blès, J.L., Coubre, C., Vuaillat, D., Gravelat, C., 1996. Rochechouart. Carte Géologique de la France. A 1/50000.

Christie, J.M., Ardell, A.J., 1974. Substructures of deformation lamellae in quartz. Geology 2, 405–408.

Désindes, L., Durand, M., Bailly, L., Jaillet, S., Bouchot, V., Lespinasse, M., Pouliquen, M., Ostermann, J.-M., Leroy, J., 2006. Genesis of the Dordogne (France) high-purity silica placers. International Journal of Earth Sciences 95, 80–94.

Dresen, G., Duyster, J., Stökhert, B., Wirth, R., Zulauf, G., 1997. Quartz dislocation microstructure between 7000 m and 9100 m depth from the Continental deep drilling program KTB. Journal of Geophysical Research 102, 18443–18452.

Drury, M.R., 1993. Deformation lamellae in metals and minerals. In: Boland, J.N., Fitzgerald, J.D. (Eds.), Defects and Processes in the Solid State: Geoscience Applications, the McLaren Volume, pp. 195–212.

Dunlap, W.J., Hirth, G., Teyssier, C., 1997. Thermomechanical evolution of a ductile duplex. Tectonics 16, 983–1000.

French, B.M., 1998. Traces of Catastrophe: a Handbook of Shock-metamorphic Effects in Terrestrial Meteorite Impact Structures. Available at:. Lunar and Planetary Institute, Houston http://www.lpi.usra.edu/publications/books/CB-954/CB-954.intro.html.

Goltrant, O., Leroux, H., Doukhan, J.-C., Cordier, P., 1992. Formation mechanisms of planar deformation features in naturally shocked quartz. Physics of the Earth and Planetary Interiors 74, 219–240.

Gratz, A.J., Nellis, W.J., Christie, J.M., Brocious, W., Swegle, J., Cordier, P., 1992. Shock metamorphism of quartz with initial temperatures −170 to +1000 °C. Physics and Chemistry of Minerals 19, 267–288.

Grieve, R.A.F., Langenhorst, F., Stöffler, D., 1996. Shock metamorphism of quartz in nature and experiment: II. Significance in geoscience. Meteoritics and Planetary Science 31, 6–35.

Heider, N., Kenkmann, T., 2003. Numerical simulation of temperature effects at fissures due to shock loading. Meteoritics and Planetary Science 38, 1451–1460.

Hirth, G., Teyssier, C., Dunlap, W.J., 2001. An evaluation of quartzite flow laws based on comparisons between experimentally and naturally deformed rocks. International Journal of Earth Sciences 90, 77–87.

Karato, S.-I., 2008. Deformation of Earth Materials. University Press, Cambridge.

Kelley, S.P., Spray, J.G., 1997. A late Triassic age for the Rochechouart impact structure, France. Meteoritics and Planetary Science 32, 629–636.

Kenkmann, T., Ivanov, B.A., Stöffler, D., 2000a. Identification of ancient impact structures: low-angle normal faults and related geological features of crater basements. In: Gilmour, I., Koeberl, C. (Eds.), Impacts and the Early Earth. Lecture Notes in Earth Sciences, vol. 91, pp. 271–309.

Kenkmann, T., Hornemann, U., Stöffler, D., 2000b. Experimental generation of shock-induced pseudotachylites along lithological interfaces. Meteoritics and Planetary Science 35, 1275–1290.

Kieffer, S.W., Phakey, P., Christie, J.M., 1976. Shock processes in porous quartzite: transmission electron microscope observations and theory. Contributions to Mineralogy and Petrology 59, 41–93.

Kraut, F., 1969. Über ein neues Impaktit-Vorkommen im Gebiete von Rochechouart-Chassenon (Départements Haute Vienne und Charente, Frankreich). Geologica Bavarica 61, 428–450.

Kraut, F., French, B.M., 1971. The Rochechouart meteorite impact structure, France: preliminary geological results. Journal of Geophysical Research 76, 5407–5413.

Küster, M., Stöckhert, B., 1999. High differential stress and low pore fluid pressure – microstructural evidence for post-seismic creep. Tectonophysics 303, 263–277.

Lambert, P., 1977. The Rochechouart crater: shock zoning study. Earth and Planetary Science Letters 35, 258–268.

Lambert, P., 1982. Anomalies within the system: Rochechouart target rock meteorite. In: Silver, L.T., Schultz, P.H. (Eds.), Geological Implications of Impacts of Large Asteroids and Comets on the Earth. Geological Society of America Special Paper, vol. 190, pp. 57–68.

Langenhorst, F., 1994. Shock experiments on pre-heated α- and β-quartz: II. X-ray and TEM investigations. Earth and Planetary Science Letters 128, 683–698.

Langenhorst, F., Deutsch, A., 1994. Shock experiments on pre-heated α- and β-quartz: 1. Optical and density data. Earth and Planetary Science Letters 125, 407–420.

Leroux, H., Doukhan, J.-C., 1996. A transmission electron microscope study of shocked quartz from the Manson impact structure. In: Koeberl, C., Anderson, R.R. (Eds.), The Manson Impact Structure, Iowa: Anatomy of an Impact Crater. Geological Society of America Special Paper, vol. 302, pp. 267–274.

Leroux, H., Reimold, W.U., Doukhan, J.-C., 1994. A TEM investigation of shock metamorphism in quartz from the Vredefort dome, South Africa. Tectonophysics 230, 223–239.

Martini, J.E.J., 1991. The nature, distribution and genesis of the coesite and stishovite associated with the pseudotachylite of the Vredefort Dome, South Africa. Earth and Planetary Science Letters 103, 285–300.

McLaren, A.C., Hobbs, B.E., 1972. Transmission electron microscope investigation of some naturally deformed quartzites. Geophysical Monograph 16, 55–66.

McLaren, A.C., Retchford, R.J.A., Griggs, D.T., Christie, J.M., 1967. TEM study of Brazil twins and dislocations experimentally produced in natural quartz. Physica Status Solidi 19, 631–644.

McLaren, A.C., Turner, R.G., Boland, J.N., 1970. Dislocation structure of the deformation lamellae in synthetic quart; a study by electron and optical microscopy. Contributions to Mineralogy and Petrology 29, 101–115.

Nüchter, J.A., Stöckhert, B., 2008. Coupled stress and pore fluid pressure changes in the middle crust: vein record of coseismic loading and postseismic stress relaxation. Tectonics 27. doi:10.1029/2007TC002180.

Pierazzo, E., Melosh, H.J., 2000. Understanding oblique impacts from experiments, observations, and modeling. Annual Review of Earth and Planetary Sciences 28, 141–167.

Poirier, J.-P., 1985. Creep of crystals – high temperature deformation processes in metals, ceramics and minerals. Cambridge University press, Cambridge. pp. 260.

Reimold, W.U., Oskierski, W., 1987. The Rb–Sr-age of the Rochechouart impact structure, France, and geochemical constraints on impact melt-target rock–meteorite compositions. In: Pohl, J. (Ed.), Research in Terrestrial Impact Structures. Friedr. Vieweg and Sohn, Braunschweig/Wiesbaden, pp. 94–114.

Robertson, P.B., 1975. Zones of shock metamorphism at the Charlevoix impact structure, Québec. Geological Society American Bulletin 86, 1630–1638.

Stipp, M., Stünitz, H., Heilbronner, R., Schmid, S.M., 2002a. The eastern Tonale fault zone: a "natural laboratory" for crystal plastic deformation of quartz over a temperature range from 250° to 700 °C. Journal of Structural Geology 24, 1861–1884.

Stipp, M., Stünitz, H., Heilbronner, R., Schmid, S.M., 2002b. Dynamic recrystallization of quartz: correlation between natural and experimental conditions. In: De Meer, D., Drury, M.R., De Bresser, J.H.P., Pennock, G.M. (Eds.), Deformation Mechanisms, Rheology and Tectonics: Current Status and Future Perspectives. Geological Society of London, Special Publication, London, pp. 170–190.

Stöckhert, B., Brix, M.R., Kleinschrodt, R., Huford, A.J., Wirth, R., 1999. Thermochronometry and microstructures of quartz – a comparison with experimental flow laws and predictions on the temperature of the brittle-plastic-transition. Journal of Structural Geology 21, 351–369.

Stöckhert, B., Duyster, J., 1999. Discontinuous grain growth in recrystallised vein quartz – implications for grain boundary structure, grain boundary mobility, crystallographic preferred orientation and stress history. Journal of Structural Geology 21, 1477–1490.

Stöffler, D., Langenhorst, F., 1994. Shock metamorphism of quartz in nature and experiment: I. Basic observation and theory. Meteoritics 29, 155–181.

Trépied, J.C., Doukhan, J.C., Paquet, J., 1980. Subgrain boundaries in quartz – theoretical analysis and microscopic observations. Physics and Chemistry of Minerals 5, 201–218.

Trepmann, C.A., 2008. Shock effects in quartz: compression versus shear deformation – an example from the Rochechouart impact structure, France. Earth and Planetary Science Letters. doi:10.1016/j.epsl.2007.11.035.

Trepmann, C.A., Stöckhert, B., 2003. Quartz microstructures developed during non-steady state plastic flow at rapidly decaying stress and strain rate. Journal of Structural Geology 25, 2035–2051.

Trepmann, C.A., Stöckhert, B., Dorner, D., Küster, M., Röller, K., Hamidzadeh Moghadam, R., 2007. Simulating coseismic deformation of quartz in the middle crust and fabric evolution during postseismic stress relaxation – an experimental study. Tectonophysics 442, 83–104.

Trepmann, C.A., Spray, J.G., 2005. Planar microstructures and Dauphiné twins in shocked quartz from the Charlevoix impact structure, Canada. In: Kenkmann, T., Hörz, F., Deutsch, A. (Eds.), Large Meteorite Impacts III. Geological Society of America, Special Paper, vol. 384, pp. 315–328.

Trepmann, C.A., Spray, J.G., 2006. Impact-related crystal–plastic processes in quartz from crystalline target rocks of the Charlevoix structure, Canada. European Journal of Mineralogy 18, 161–173.

Trepmann, C.A., Stöckhert, B., 2001. Mechanical twinning of jadeite – an indication of synseismic loading beneath the brittle–ductile transition. International Journal of Earth Sciences 90, 4–13.

Trepmann, C.A., Stöckhert, B., 2002. Cataclastic deformation of garnet: a record of synseismic loading and postseismic creep. Journal of Structural Geology 24, 1845–1856.

Voll, G., 1976. Recrystallization of quartz, biotite and feldspars from Erstfeld to the Leventina nappe, Swiss Alps, and its geological significance. Schweizer mineralogische und petrographische Mitteilungen 56, 641–647.

White, S., 1973. Deformation lamellae in naturally deformed quartz. Nature Physical Science 245, 26–28.

White, S., 1975. The effects of polyphase deformation on the intracrystalline defect structures of quartz. II. Origin of the defect structures. Neues Jahrbuch der Mineralogie, Abhandlungen 123, 237–252.